8. At the deepest layers monitored—i.e., 99 to 130 cm (39 to 51 in) for the flexible pavement and 38 to 61 cm (15 to 24 in) for the rigid pavement—the responses to various modes of aircraft operation of the flexible and rigid pavements were 10 and 30 percent respectively of their surface responses.

9. Elastic and inelastic displacement behavior and response can be accurately modeled mathematically.

10. The elastic and inelastic displacement behavior directly correlates the behavior of the WES pavement test sections under simulated aircraft loads and wheel configurations and distributed (not conditioning) traffic to the behavior of an actual pavement under actual aircraft operations (NAFEC tests). This correlation means that any further investigation of dynamic load effects can probably be conducted on pavement test sections of limited size.

11. Inelastic behavior occurred in both the nonconditioned flexible and the rigid pavement structures and may possibly be a common characteristic that links the performance of all types of pavement. In fact, it may be the major controlling factor or mechanism for pavement performance and life because it can be the primary movement for static and low-speed operations.

RECOMMENDATIONS

The thickness required of pavements subjected to parked or slow-moving aircraft should be based on the static mass of the aircraft, as is the current practice. This applies to the parking aprons, taxiways other than high-speed exit areas, and runway ends. In high-speed exit areas, runway interiors, and other areas that are subjected to high-speed aircraft operations only, the design should be based on an analysis of the design loading to the pavement and the pavement response to dynamic loading. In high-speed exit areas, high horizontal loads are applied to the pavement surface and should be considered in the design. Because of the large loads and thus the likelihood of excessive deterioration in turn areas, the pavement surface in exit areas of flexible pavement runways should be strengthened or be stronger than the main runway. In runway interiors, the NAFEC test data indicate that thickness reductions could be considered. However, to take full advantage of the NAFEC test data in pavement design, more knowledge is needed concerning pavement failure mechanisms and deterioration growth functions and causes.

ACKNOWLEDGMENT

This paper is a summary of a series of reports to FAA (1, 2, 3).

REFERENCES

1. F. Horn and R. H. Ledbetter. Pavement Response to Aircraft Dynamic Loads: Instrumentation Systems and Testing Program. Federal Aviation Administration, Rept. FAA-RD-74-39-1, June 1975; NTIS, Springfield, VA, ADA-016-450.
2. R. H. Ledbetter. Pavement Response to Aircraft Dynamic Loads: Presentation and Initial Analysis of Data; Appendix A—Automatic Data Processing; Appendix B—Data. Federal Aviation Administration, Rept. FAA-RD-74-39-2, Sept. 1975.
3. R. H. Ledbetter. Pavement Response to Aircraft Dynamic Loads: Compendium. Federal Aviation Administration, Rept. FAA-RD-74-39-3, June 1976.

Dynamic Response of Aircraft to Pavement Unevenness

Anthony G. Gerardi, Wright-Patterson Air Force Base, Ohio

A computer program was developed to simulate aircraft dynamic response to runway roughness during taxiing and takeoff. The mathematical model has rigid-body degrees of freedom of pitch, roll, and vertical and horizontal translation and up to 30 flexible modes of vibration. Runway profile data measured at approximately 0.61-m (2-ft) intervals is input into the program and used as the model forcing function. A different profile is encountered by each landing gear. All the necessary landing-gear and airplane data were collected for the following aircraft: Boeing—KC-135; B-52C,G,H; T-43 (737); AMST Comp (YC-14); 727-100; 727-200; 707-320; and 747; McDonnell Douglas—AMST Comp (YC-15); C-9A,B; DC-8-63; DC-9-40; DC-10-10; and RF-4C; Lockheed—C-130E; C-5A; C-141; and L-1011; and other—F-111A; A-37; and CT-39. Each of these aircraft was simulated; a comparison of the responses of several different military aircraft showed that the simulated accelerations at the pilot stations were within 5 to 10 percent of the measured values. Typical computer run times were less than 60 s on a CDC 6600. The intended purpose of the program was to locate the rough areas of a runway by using the ±0.4*g* criterion as a limiting vertical acceleration. Additional useful applications of the program are (a) analysis of pavement dynamic loading; (b) runway repair evaluation; (c) evaluation of the dynamic response of new aircraft, such as the Concorde and supersonic transport, on a given runway profile; and (d) the performance of aircraft parametric studies, such as that of the high preload-pressure, nose landing-gear strut, to determine methods for reducing aircraft ground loads.

The problem of pavement unevenness is of concern to many persons in the airport and aircraft industries: Runway contractors are required to build smoothness into new and overlaid runways. Airport owners and operators are required to ensure that smoothness is maintained. Aircraft manufacturers are required to design their aircraft with good ride quality and structural integrity for both air and ground operations. One of the objects of each is to minimize aircraft structural damage and passenger and crew discomfort during ground operations.

Figure 1 (1) shows the derivation of the current roughness criterion used to set maximum allowable levels of vertical acceleration. This is a human-comfort, rather than an aircraft structural, criterion. Most current passenger aircraft have rigid-body natural frequencies of less than 10 cycles/s. At these frequencies, the acceleration-versus-frequency curve is relatively flat and corresponds to a value of approximately ±0.4 *g*. Essentially then, if the vertical acceleration level at any point along the fuselage exceeds ±0.4 *g*, measured from zero to peak, that particular section of that runway is too rough for that particular aircraft. Next, a technique for determining when the acceleration-criterion level has been exceeded must be established. There are two basic methods for this: aircraft instrumentation and testing or aircraft simulation.

Aircraft testing requires the instrumentation of an aircraft, the calibration of the instrumentation, and data reduction and interpretation. It involves expensive

equipment and skilled operators and is time-consuming. Also, when a given runway that is suspected of being excessively rough is being evaluated in this manner, each of the types of aircraft that operate on it must be tested because each type of aircraft will respond differently.

The second method, aircraft simulation, requires detailed aircraft and runway-profile data and mathematically simulates an aircraft traversing a runway by using a digital computer.

This paper describes the formulation of one such computer program and how it can be used to help solve pavement-unevenness problems.

GENERAL AIRPLANE AND RUNWAY MODEL

The general mathematical model is represented as an asymmetrical body with a nose and a right and a left main landing gear. Each landing-gear strut is assumed to have point contact with the profile, and it is assumed that each landing gear traverses a different profile. The model has aerodynamic lift and drag and thrust applied at the center of gravity of the aircraft.

The aircraft is free to roll, pitch, plunge, and translate horizontally down the runway, and each landing-gear unsprung mass is free to translate vertically. In addition to these rigid-body degrees of freedom, there are up to 30 flexible modes of vibration. This aircraft motion is controlled by the landing-gear strut forces and the lift, drag, thrust, and resisting parameters of aircraft mass and inertia.

The landing-gear struts are nonlinear, single- or double-acting, oleopneumatic energy-absorbing devices (Figure 2) and are represented in the model as the sum of the three forces—pneumatic, hydraulic, and strut bearing friction. The pneumatic force (F_A), which is the largest of the three, is given for a single-chambered strut by Equation 1.

$$F_A = PV/[(V/A) - S] \tag{1}$$

where

P = pressure of fully extended strut,
V = volume of fully extended strut,
A = pneumatic-piston area, and
S = strut stroke.

The hydraulic or damping force (F_h) is given by Equation 2.

$$F_h = \rho_h A_h^3 \dot{S}|\dot{S}|/2(C_d A_o)^2 \tag{2}$$

where

ρ_h = density of hydraulic fluid,
A_h = hydraulic-piston area,
A_o = effective orifice area (constant orifice minus metering-pin area),
C_d = orifice coefficient (usually 0.9), and
$\dot{S}$ = strut-piston velocity.

The strut bearing-friction force (F_F) is given by Equation 3.

$$F_F = (\mu|F_u| + \mu|F_l|) \times \dot{S}/|\dot{S}| \tag{3}$$

where

μ = sliding coefficient of friction (usually 0.1),
F_u and F_l = upper and lower bearing forces required to balance lateral loading,

and

$$F_l = F_s X_a/(X_b + S) \tag{4}$$

and

$$F_u = 1.0 - [X_a/(X_b + S)] \tag{5}$$

where

F_s = total wheel-drag force,
X_a = strut-piston length, and
X_b = minimum bearing separation.

The force F_s can be large during landing spin-up or braking. During taxiing, however, it is very small compared to the total strut static force for symmetrically loaded struts and, for this reason, is usually neglected in the simulation.

The tire force (F_{T1}) is given by Equation 6.

$$F_{T1} = kT_D \tag{6}$$

where T_D = tire deflection and k = linear tire-spring constant.

The runway elevation data (Figure 3) are input into the model in 0.61-m (2-ft) long increments. The profile is made continuous by fitting the following polynomial through three points and the slope at the end of the previous profile segment:

$$y(x) = a_1 + a_2 x + a_3 x^2 + a_4 x^3 \tag{7}$$

where a_1, a_2, a_3, and a_4 = coefficients derived from elevation and slope data. This is done for each of the three lines of runway-profile data.

Rigid-Body Equations of Motion

The differential equations of motion for the mathematical model were derived by Lagrange's method. The general form is given by Equations 8 through 14 and corresponds to the notation shown in Figure 4; i.e., $\ddot{Z}$, $\ddot{\theta}$, $\ddot{\phi}$, and $\ddot{X}$ = center-of-gravity vertical, and pitching, rolling, and horizontal accelerations respectively.

$$\ddot{Z} = (F_{s1} + F_{s2} + F_{s3} + L - W)/M_{cg} \tag{8}$$

(The subscripts 1, 2, and 3 correspond to the nose and right and left main landing gears respectively.)

$$\ddot{Z}_1 = (F_{t1} - F_{s1} - W_1)/M_1 \tag{9}$$

$$\ddot{Z}_2 = (F_{t2} - F_{s2} - W_2)/M_2 \tag{10}$$

$$\ddot{Z}_3 = (F_{t3} - F_{s3} - W_3)/M_3 \tag{11}$$

$$\ddot{\Theta} = (F_{s1}A + F_{s2}B + F_{TD}\epsilon_1 - F_{s3}C)/I_{yy} \tag{12}$$

$$\ddot{\phi} = (F_{s3} - F_{s2})C/I_{xx} \tag{13}$$

$$\ddot{X} = (F_T - F_{TD} - F_{AD})/(M_{cg}) \tag{14}$$

where

F_{s1}, F_{s2}, and F_{s3} = total landing-gear strut forces,
F_{t1}, F_{t2}, and F_{t3} = tire forces,
M_{cg} and W = aircraft mass and deadweight,
I_{yy} and I_{xx} = aircraft pitch and roll inertias,
W_1, W_2, and W_3 = unsprung landing-gear masses,
A, B, C, and ϵ_1 = moment arms,
F_T = thrust, and
F_{TD} and F_{AD} = tire and aerodynamic drag forces.

(F_T and F_{AD} act through the center of gravity.)

Flexibility Equations of Motion

The modal analysis technique is used to describe the flexible motion of the aircraft, as shown by Equation 15.

$$M_i q_i = \xi_{i1} F_{s2} + \xi_{i2} F_{s2} + \xi_{i3} F_{s3} - 2\zeta_i \omega_i \dot{q}_i - \omega_i^2 M_i q_i \quad \text{(for i th mode)} \quad (15)$$

where

M_i = generalized mass;
ξ_{i1}, ξ_{i2}, and ξ_{i3} = modal deflections at gear locations 1, 2, and 3;
ω_i = modal frequency;
ζ = damping factor; and
q_i, $\dot{q}_i$, and $\ddot{q}_i$ = generalized coordinates and their time derivatives.

The sign convention is as follows:

Sign	Motion	Convention
Z	Vertical displacement	+ = up
Θ	Pitch	+ = nose down
ϕ	Roll	+ = roll right
q	Deflection due to bending	+ = up
X	Horizontal translation	+ = forward

Figure 1. Accepted military criterion for human tolerance of vertical vibration.

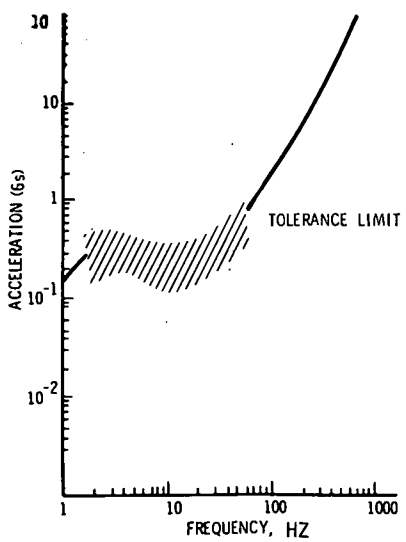

Figure 2. Single-acting oleopneumatic landing-gear strut.

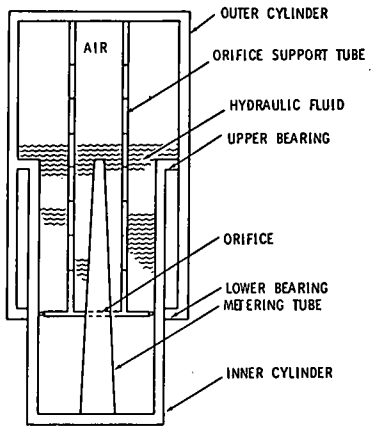

Figure 3. Runway profile representation.

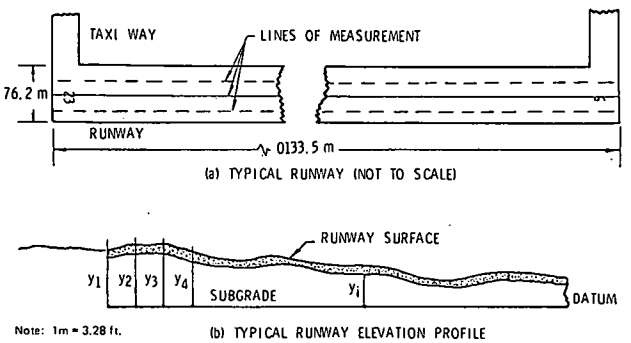

Figure 4. Asymmetrical mathematical model.

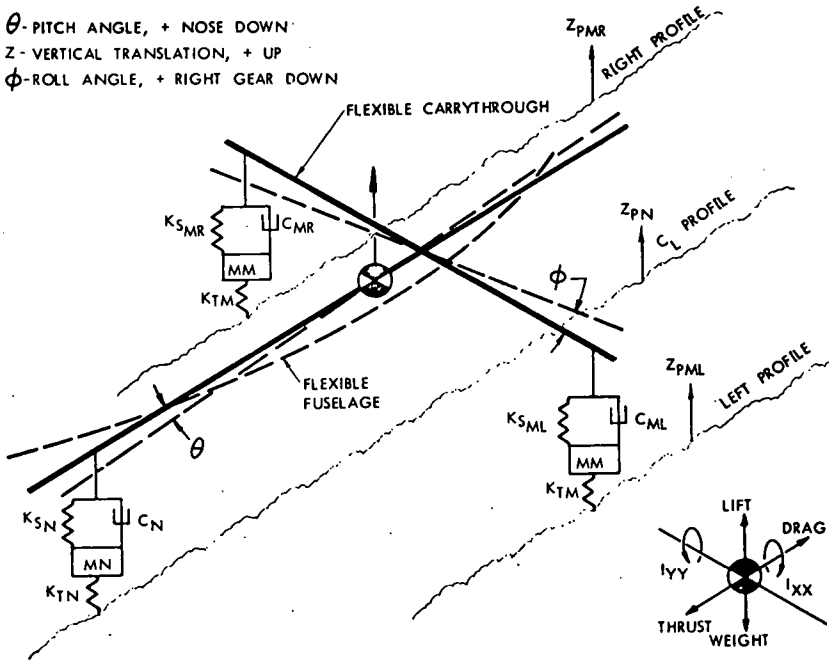

Figure 5. Typical Calcomp-plotted output.

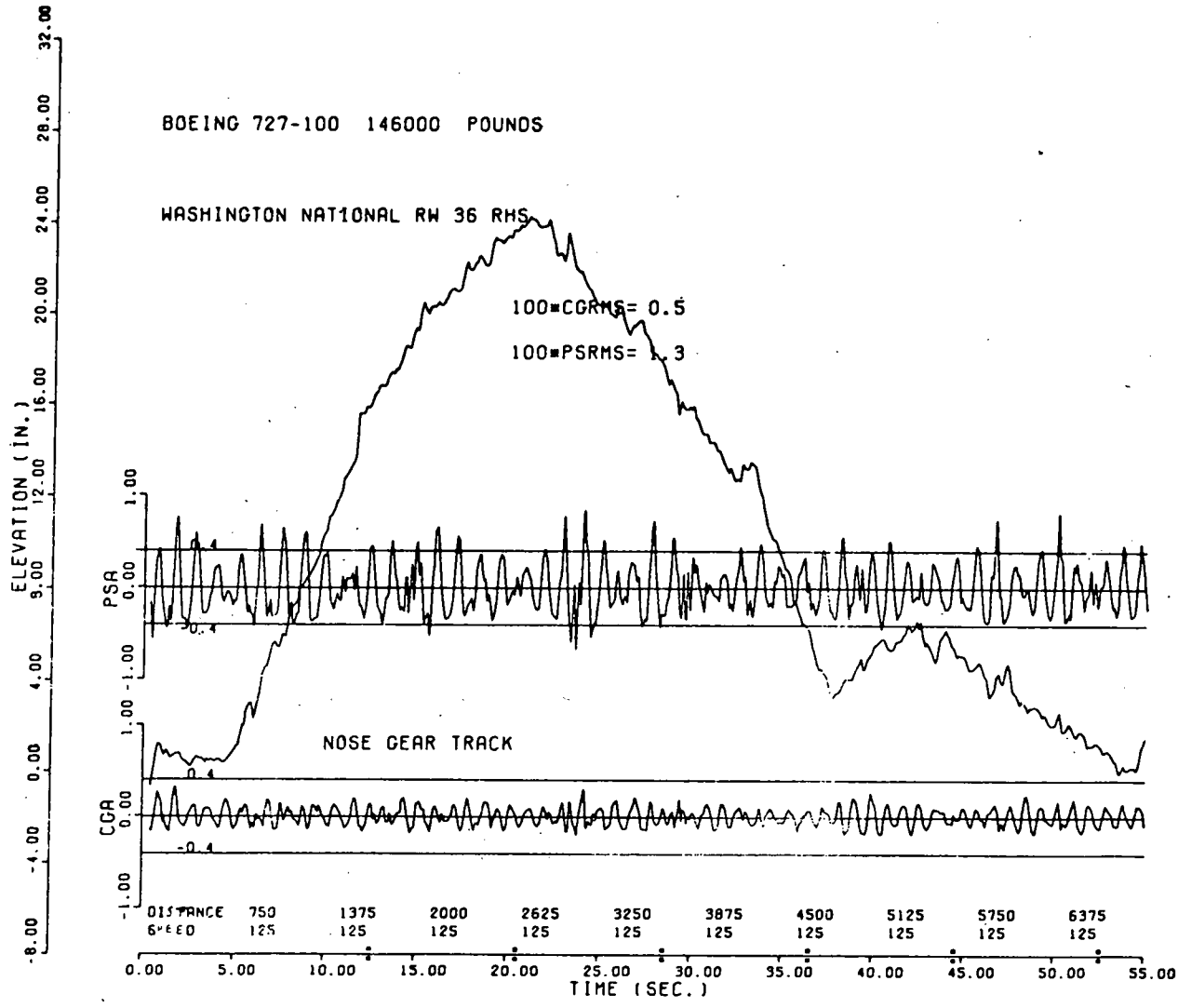

Figure 6. Simulated and measured time histories of center-of-gravity acceleration of C-41 traversing bump.

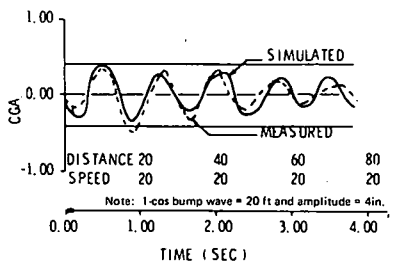

Solution Technique

The coupled nonlinear differential equations of motion that describe the simulated aircraft were solved by using a three-term Taylor series technique. For example, for the general equation

$$\ddot{x} = -c\dot{x} - kx' \tag{16}$$

the three-term Taylor series representation can be written as

$$x_{(I+1)} = x_{(I)} + \dot{x}_{(I)}(\Delta t) + \ddot{x}_{(I)}(\Delta t)^2/2 \tag{17}$$

where I = varies between 1 and N. The values of $\ddot{x}$, $\dot{x}$, and x from one step are substituted into Equation 17 and a new value of x is obtained. Then, differentiating Equation 17 gives the velocity $\dot{x}$; i.e.,

$$\dot{x}_{(I+1)} = \dot{x}_{(I)} + \ddot{x}_{(I)}(\Delta t) \tag{18}$$

The values of $\dot{x}$ and $\ddot{x}$ from the previous equation are substituted into Equation 18 and a new value of $\dot{x}$ is found. This entire process is repeated with the new values of x and $\dot{x}$ to obtain the next point in the solution.

RESULTS

The results of the computer program are provided as both a printed output and a time-history plot. The printed output lists the following parameters at time intervals of 0.01 s.

Parameter	Description
XMAINL	Left main-landing-gear strut deflection (in)
XMAINR	Right main-landing-gear strut deflection (in)
ZPML	Left main-landing-gear runway elevation (in)
ZPMR	Right main-landing-gear runway elevation (in)
ZPN	Nose-landing-gear runway elevation (in)
BETADD	Rolling acceleration ($\ddot{\phi}$) (rad/s^2)

Figure 7. Effect of nose-strut preload pressure: (a) 813.5 kPa and (b) 2068.2 kPa.

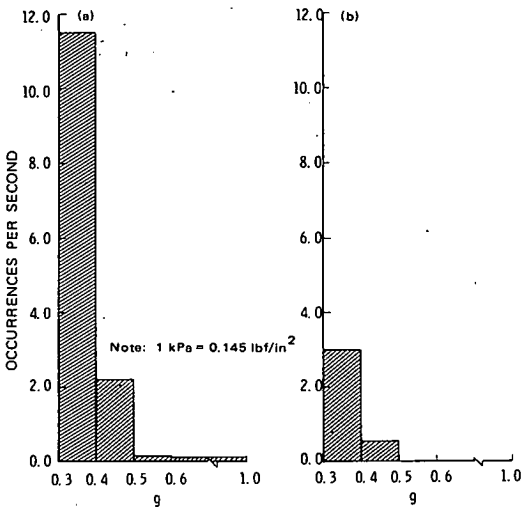

Parameter	Description
THETADD	Pitching acceleration ($\ddot{\Theta}$) (rad/s^2)
BETA	Roll angle (ϕ) (rad)
THETA	Pitch angle (Θ) (rad)
SPEED	Aircraft velocity (ft/s)
DISTANCE	Distance traveled down runway (ft)
TIME	Real time (s)
CGACC	Center-of-gravity vertical acceleration (g)
PSA	Pilot's station vertical acceleration (g)

(This model was designed for U.S. customary units only; therefore, values in Figure 5 and the following discussion are not given in SI units.)

Figure 5 shows a reduction of a typical Calcomp-plotted time history that depicts a Boeing 727-100 taxiing at 125 ft/s over the runway 36 profile at Washington National Airport. The plotted output includes titles showing the airplane simulated, its gross mass, the runway number, and its location. The abscissa is the time axis annotated every second. At every time annotation, the current value of the aircraft speed and the current aircraft position on the runway are printed out. The runway markers are also plotted on the time scale to aid in aircraft positioning. In this figure, the nose-gear track is a time history of the runway profile as it is encountered by the nose gear of the aircraft. The actual runway profile is preceded by 100 ft of smooth surface to allow any model transients to damp out before encountering the actual profile. There are two aircraft-acceleration time histories—that at the pilot's station (PSA) and that at the center of gravity (CGA) of the aircraft. Each time history is banded by the human tolerance criterion of $\pm 0.4\,g$. To minimize the amount of core required to store the acceleration time histories, the higher frequency components were effectively filtered out by limiting the sampling interval. All of the acceleration peaks, however, are shown. The PSA time history is not always within the band of the accepted human-tolerance criteria. Thus, the plot is useful in that it provides a graphical record of the level of acceleration and shows which bumps in the runway profile caused the high acceleration response.

The following comparisons of simulated to measured response were made with four different aircraft. (In these simulations, a computer program was used that differed from the one described above in that it did not have a roll degree of freedom and used only one set of runway profile data.)

1. The simulated response of a 273 000-lb KC-135 aircraft taking off from runway 05 at Torrejon Air Force Base in Spain easily identified the rough section of the runway.
2. The simulated response of a B-52 heavy (400 000-lb) bomber at a constant 40-knot taxi speed on runway 18 at U-TAPAO Air Force Base in Thailand identified the rough section of the runway; the peak acceleration levels were within 6 percent of the measured levels.
3. The simulated response of a 37 636-lb F-4C aircraft operating at a constant 29-knot taxi speed over a bomb repair patch 4.6 m (15.5 ft) long and having a maximum amplitude of 3.8 cm (1.5 in) at Wright-Patterson Air Force Base in Ohio had peak acceleration levels at the center of gravity of the aircraft that were within 9 percent of the measured levels.
4. The simulated response of a 304 000-lb C-141 aircraft operating at a constant 12-knot taxi speed had peak acceleration levels that were within 11 percent of the measured levels; this is shown in Figure 6.

For most cases, the simpler program is sufficient for simulating an aircraft operating from paved surfaces. However, the advent of the advanced medium STOL transport (AMST), where operations from rough or totally unprepared fields are required, made it necessary to add the roll degree of freedom and use the three sets of runway profile data.

Comparisons of the improved version of the computer program with measured data have not yet been made, but it is expected that the added sophistication of the program will improve its accuracy.

The detailed airplane data required to accurately describe the aircraft being simulated are summarized below:

1. General airplane data—thrust, weight, inertia, center of gravity, and landing-gear locations;
2. Airplane flexibility data—generalized mass and frequencies and modal deflections at each gear, the center of gravity, the tail, and the pilot's station; and
3. Landing-gear data—weight of unsprung mass, strut and tire pressures, piston areas, strut volumes and strokes, and detailed description of fluid metering device.

These data have been collected and simulations have been made for the following aircraft:

Boeing	McDonnell Douglas	Lockheed	Other
KC-135	AMST Comp (YC-15)	C-130E	F-111A
B-52C,G,H	C-9A,B	C-5A	A-37
T-43 (737)	DC-8-63	C-141	CT-39
AMST Comp (YC-14)	DC-9-40	L-1011	B-1
727-100	DC-10-10		
727-200	RF-4C		
707-320			
747			

The final information required for the simulation is the three lines of runway profile data. An elevation point is required every 0.61 m (2 ft) for each line of survey. The Air Force Weapons Laboratory has developed and is using a device known as a laser profilometer that measures runway profiles quickly and accurately and in a form compatible with the computer simulation requirements.

CONCLUSIONS

A computer program has been developed that can analytically determine whether the dynamic response of an aircraft to a given runway profile exceeds the established roughness criteria of ±0.4 *g* and locate these rough areas on the runway.

1. Use: The program is general and will simulate most current commercial and military aircraft. The necessary data have already been assembled for many of these aircraft.
2. Efficiency: A C-9A takeoff simulation requires 70 s of central processing unit time on a CDC 6600 digital computer. This is just 30 s over real time and a number that is typical for all simulations.
3. Loads incurred on pavement: It would be easy to plot time histories of pavement loading rather than of aircraft vertical accelerations.
4. Aircraft parametric studies: The program can be used to perform parametric studies on aircraft to determine methods of reducing ground loads by modification of the aircraft.

One good example of a parametric study is the soft nose strut study, which found that by increasing the strut preload pressure of the nose landing gear, the vertical acceleration levels at the pilot's station were reduced significantly. This idea was tested with a Boeing 727-100 at Oklahoma City. The peak acceleration at the pilot's station was cut from 2 *g* peak to peak to 1 *g*.

Figure 7 shows a histogram of the data from the taxi runs made at Oklahoma City; the overall aircraft response was significantly reduced throughout the entire test.

5. Accuracy: The comparison of the computed to the measured peak-vertical-acceleration levels was very good for all aircraft.
6. In addition to the identification of rough areas on runways, the program has other potential uses: i.e., runway repair evaluation—the program can be used to determine the minimum amount of repair required to bring the runway to acceptable standards from an aircraft-response standpoint—and prediction of response of other aircraft—the program can be used to predict the dynamic response of aircraft that will operate from a given runway in the future (e.g., a runway that is marginal for a Boeing 727 or a DC-8 may be unacceptable for the Concorde or a supersonic transport).

Abridgment

Analysis of Airport Runway Roughness Criteria

Paul N. Sonnenburg, Civil Engineering Research Facility, University of New Mexico

In this work, attention is focused on runway surface roughness and its effect on aircraft vibrational responses that, in turn, affect passenger comfort. The basic problem is to develop a method for determining quantitatively when and precisely where a runway is too rough. The object is to be able to provide airport operators with sufficiently detailed information for the authorization of adequate repairs at minimum costs.

RECOMMENDED PROCEDURE

The recommended procedure is that a statistical analysis of profile data be used to establish a roughness criterion. This implies that aircraft-vibration-response data need not be considered in establishing roughness criteria, even though these data can provide supporting evidence of the degree of roughness. Hence, the aircraft itself is not a factor in the recommended approach. The statistical analysis of profile-elevation data is possible if the data are filtered to remove the elevation trends that are formed by long wavelengths. A profile can then be rated according to its overall and its detailed roughness properties. The standard deviation of displacement (σ) is recommended as an overall index, and the standard deviations of the slopes and the slope changes might be considered as detailed indexes (extremal analysis). The detailed roughness properties are necessary because a profile may be generally smooth, yet have a few severe bumps. The statistical approach discussed here addresses only the determination of the standard deviation of displacement as an overall index; additional work is recommended. Finally, when all known indexes are extracted from the profile data, each should be correlated with subjective pilot ratings, and those showing the strongest agreement should be emphasized.

APPROACHES

The first indications of runway surface roughness are often verbal complaints by pilots. For this reason, the first roughness criterion investigated was human vibration. Human-response curves indicate that a peak vibration-acceleration level of about 0.4 *g* from about 2.0 to 20.0 Hz can be tolerated for at least 5 min, with a broad band of statistical scatter about this level. There are some theoretical and experimental data that show a few isolated peaks that reach or exceed 0.4 *g* on runways claimed to be rough by pilots. However, the existence of peaks only implies intermittent, rather than continuous, exposure, and it was therefore concluded that other sources of human-response data would be needed to establish a criterion.

In a second effort, an absorbed-power approach was investigated. A human can absorb 6 W of vibrational power for extended periods of time (1 or more min). However, for taxiing aircraft, the absorbed power exceeds 6 W for one or two approximately 5-s intervals during an entire run and, again, this occurs occasionally rather than continuously. Furthermore, the peak power is a function of the time interval over which the power is averaged. For example, if a 20-W peak for 1 s is averaged over 1 min, the resulting power level is negligible so that a rationale for establishing a power-averaging approach does not exist. The absorbed-power approach is more useful in locating rough regions than is the 0.4 *g* approach, but it still cannot be used to locate rough points precisely.

The third approach, using human criteria, was suggested by data from the Aerospace Medical Research Laboratory (AMRL) at Wright-Patterson Air Force Base, Ohio. These data were in disagreement with the absorbed-power results, and the 0.4 *g* criterion was con-